Sources and Coded Aperture Transmittance Analysis in Compressive Computed Tomography[1]

Análisis del número de fuentes y transmitancia de aperturas codificadas en tomografía computarizada compresiva[2]

Óscar Espitia Mendoza[3]
Yuri Mejía Melgarejo[4]
Henry Argüello Fuentes[5]

doi:10.11144/Javeriana.iyu20-2.scaa

How to cite this article:
O. Espitía Mendoza, Y. Mejía Melgarejo, and H. Argüello Fuentes, "Sources and coded aperture transmittance analysis in compressive computed tomography," *Ing. Univ.*, vol. 20, no. 2, pp. 411-431, 2016. doi:10.11144/Javeriana.iyu20-2.scaa

[1] Submitted on: March 9th, 2015. Accepted on: March 8th, 2016. This article is derived from the research project *Diseño y simulación de una arquitectura de tomografía computarizada para el sensado compresivo de imágenes de rayos-X,* code number VIE 1803 1803, developed by the research group Diseño de Algoritmos y Procesamiento de Datos Multidimensionales of the Universidad Industrial de Santander, Bucaramanga, Colombia.

[2] Fecha de recepción: 9 de marzo de 2015. Fecha de aceptación: 8 de marzo de 2016. Este artículo se deriva de un proyecto de investigación denominado *Diseño y simulación de una arquitectura de tomografía computarizada para el sensado compresivo de imágenes de rayos-X* , código VIE 1803, desarrollado por el grupo de investigación en Diseño de Algoritmos y Procesamiento de Datos Multidimensionales de la Universidad Industrial de Santander, Bucaramanga, Colombia.

[3] Ingeniero de sistemas. Estudiante de Maestría en Ingeniería de Sistemas e Informática, Universidad Industrial de Santander, Bucaramanga, Colombia. E-mail: oscar.espitia@saber.uis.edu.co

[4] Ingeniera electrónica, magíster en Ingeniería Electrónica. Estudiante del Doctorado en Ingeniería Electrónica, Universidad Industrial de Santander, Bucaramanga, Colombia. E-mail: yuri.yejia@saber.uis.edu.co

[5] Ingeniero electricista. Magíster en Potencia Eléctrica, Universidad Industrial de Santander, Bucaramanga, Colombia. PhD in Electrical and Computer Engineering. Profesor titular de la Universidad Industrial de Santander. E-mail: henarfu@uis.edu

Abstract

Computed tomography (CT) allows the three-dimensional internal structure reconstruction of an object illuminated with X-ray light. In CT, a set of two-dimensional projections are taken to reconstruct the underlying object structure. The number of projections needed for sensing a CT scene is determined by the Nyquist limit. In some cases, the imposed projections number is excessive. Compressive sensing (CS) has emerged as a new sampling technique requiring fewer projections than those specified by the Nyquist criterion. Instead of measuring the samples directly, they are encoded before being integrated into the detector. This paper describes a CS system for CT based on coded apertures. An optimized value of transmittance and an aperture distribution are selected such that the quality of reconstruction is maximized. Simulations show that results in reconstruction with 50% of measurements are comparable with the traditional CT method based on Nyquist criterion. Similarly, results indicate that the PSNR of reconstructed images can be controlled according to the number of projections taken.

Keywords

computed tomography; compressive sensing; x-rays; coded aperture; transmittance

Resumen

La tomografía computarizada (TC) permite la reconstrucción tridimensional de la estructura interna de un objeto que es iluminado con rayos X. En TC se toman un conjunto de proyecciones bidimensionales para luego reconstruir la estructura del objeto. El número de proyecciones necesarias para realizar el muestreo de una escena en TC se determina por el límite de Nyquist. En algunos casos, el número de proyecciones impuestas es excesivo. El muestreo compresivo (CS) ha emergido como una nueva técnica de muestreo que requiere un número menor de proyecciones que las especificadas por el criterio de Nyquist. En lugar de medir las muestras directamente, en CS, son codificadas antes de integrarse en el detector. En este trabajo se describe un sistema de CS para TC basado en aperturas codificadas. Se realiza la selección de los valores óptimos de transmitancia y la distribución de aperturas que garantizan una reconstrucción eficiente. Las simulaciones realizadas muestran que los resultados de las reconstrucciones con el 50% de las medidas son comparables con las del método tradicional. Igualmente, los resultados indican que las imágenes reconstruidas tienen un PSNR que puede controlarse de acuerdo con el número de proyecciones tomadas.

Palabras clave

tomografía computarizada; muestreo compresivo; rayos X; apertura codificada; transmitancia

Introduction

Computed tomography (CT) is a technology established for the non-invasive acquisition of images from the internal structure of the objects in three dimensions (3D) [1]. In CT, an object can be reconstructed from a set of two-dimensional projections, which are produced by illuminating the object with an X-ray source. CT is important for medical diagnosis and its applications address several areas of industry, material science, biophysics, among others [2]-[4].

The CT image reconstruction algorithms have been restricted by the Nyquist theorem [5]; thus, in some CT applications, the established number of projections is excessive since high X-ray dose could be destructive or carcinogenic for human beings [6]. For this reason, it appears the interest to find acquisition methods for reducing the object exposure to the X-ray radiation, without sacrificing the quality of the images.

Furthermore, compressed sensing (CS) has recently emerged as a branch of signal processing. It is based on the fact that many signals in nature can be represented by a few coefficients in some representation basis [7]. In CS, the samples are coded in order to reduce the data redundancy in a scene; these coded measurements are enough to reconstruct the signal with a comparable quality of the signal sampled following the Nyquist theorem [8].

Data reconstruction in traditional CT is performed from projections obtained in a detector that measures the X-ray attenuation after they pass through the object. To implement the CS theory in a CT configuration it is possible to include coded apertures that allow coding the measurements to take compressed samples. Coded apertures are two-dimensional arrays with patterns of opaque materials; sections that do not contain opaque material define the transmittance of the aperture, that is, the light fraction that can pierce them [7]. In CT, this parameter can define the quantity of radiation that the object receives from each projection.

Some works have focused on developing models for joining CS to CT [9]-[11]. Nevertheless, the measurement architectures design to improve the quality of

the reconstructions has not been detailed. In this work, a multisource CT system is designed from a measurement matrix model by using CT theory and the sampling principle of coded measurements, thus, the geometry of the architecture is described and an analysis of the parameters of coded apertures and number of X-ray sources are performed to ensure efficient tomography reconstruction. In order to specify the results, this study is organized as follows: Section 1 explains in detail the traditional acquisition model, compressed sensing theory, and the proposed model; Section 2 brings coded apertures design; Section 3 describes reconstruction algorithms; Section 4 shows simulations results, and finally, the discussion section is presented.

1. Acquisition Methods

Traditional CT method (known as transmission CT) is based on estimating the X-ray attenuation after the rays pass through the underlying object [1]. In the last few years, some methods to measure changes in the X-ray intensity have been developed . These methods use multiple sources and optical instruments which modulate the beams to improve quality and to reduce the radiation dose.

Recently, systems based on the influence of the number of X-ray sources over CT reconstructions have been proposed. For instance the systems, *Pioneering Dynamic Spatial Reconstruction of Mayo Clinic* [12], *Line Sources* CT [13], *Inverse-geometry* CT, and *Ultimately a rebirth of stationary* CT [14] have multiple X-ray sources distributed in different ways. The usage of more sources allows reducing the data acquisition time, decreasing the radiation dose, and increasing the spatial resolution of images and reconstruction accuracy. Although developments of acquisition technologies have centered on detection systems, it is expected that the next advance focuses on the use of multiple X-ray sources [15].

On the other hand, compressive sensing technique has been used for transmission CT reconstruction, and thus Compressive CT (CCT) method has been established. CCT is investigated in multisource systems [10]. The implementation of CS in CT seeks to reduce the number of measurements in the sampling process without risking the image quality. In the next subsections, the measure acquisition model in CT and CS is detailed and the CCT experimental system is also detailed.

1.1. Transmission CT

Figure 1 shows an object Q discretized when it is lightened with X-rays from a source S. This representation is composed of voxels that form Q_1 cross-sections

or slices, each one with $Q_2 \times Q_3$ superficial dimensions. For each voxel (with dimensions $d_x \times d_y \times d_z$) an attenuation μ is allocated.

Figure 1. Diagram of a cone beam flat panel X-ray transmission system. *S* is an X-ray source, *Q* is an object, *D* is a detector array (flat panel detector), I_0 and *I*(*x*) are initial and measured intensities, respectively

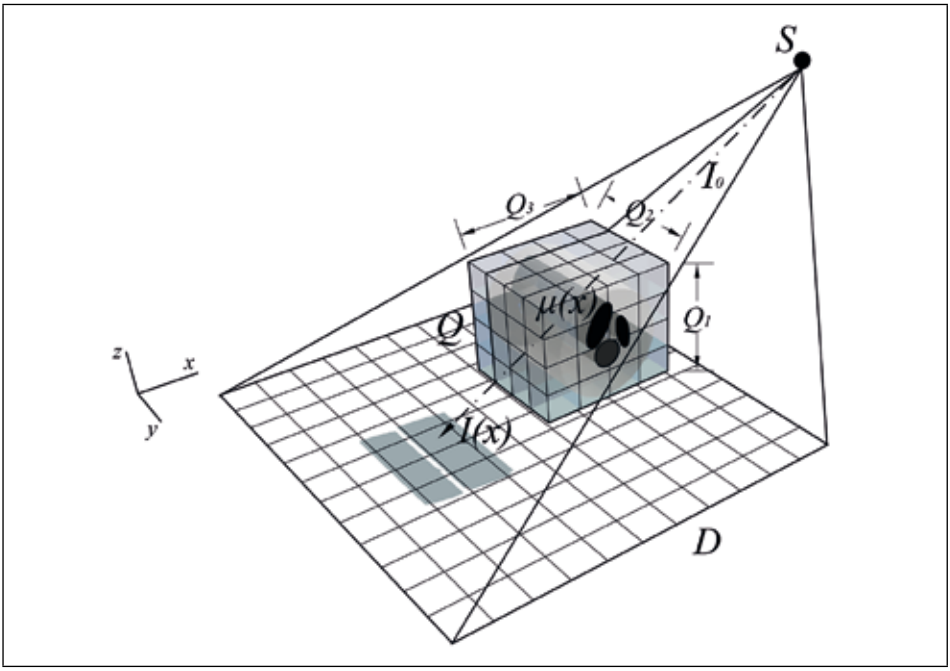

Source: authors' own presentation

Considering a ray with intensity I_0, which passes through the object with a non-homogeneous attenuation distribution $\mu(x)$, the ray intensity $I(x)$ measured by the detector D depends on the distance x passed through and the attenuation $\mu(x)$ of each point in its trajectory. This can be modeled as:

$$I_{(x)} = I_0 e^{-\int_L \mu(x)dx} \tag{1}$$

This phenomenon obeys Lambert Beer's law, and can be rewritten as:

$$-\ln\left(\frac{I(x)}{I_0}\right) = \int_L \mu(x)dx \tag{2}$$

Eq. (2) is described as the fraction of transmitted light through the object and it can be assigned to a one-dimensional projection, received with regard to an angle of incidence. Reconstruction lies in estimating the distribution of the attenuation coefficients $\mu(x)$ from that information [1].

1.2. Compressive Sensing

Compressive sensing (CS) is a new theory to acquire and to reconstruct a signal efficiently by searching a sparse solution to an underdetermined system of linear equations [16]. As opposed to the traditional signal acquisition process, CS allows sampling rates close to signal intrinsic information rate, which is much lower than Nyquist criteria.

The CS theory is based on two conditions principally: (1) the sparsity of digital signals and (2) the incoherence of the measurement matrix which depends on the sensing trajectory [17].

An image is sparse if the most of its elements are close or are equal to zero. Assuming a linear measurement process that calculates $M \ll N$ internal products between f and a collection of vectors $\{\phi_j\}_{j=1}^{M}$, as $y_i = \langle f, \phi_j \rangle$, then,

$$y = \Phi f, \tag{3}$$

where the set of y_i projections form the vector y of M elements, $\Phi \in \mathbb{R}^{M \times N}$ is the measurement matrix, ϕ_j^T is the jth row of Φ, and f is the underlying signal. Taken into account the reconstruction of f from y, it is known that there exist infinite solutions for the equation (3), because the dimensionality of y is much lesser than the dimensionality of f. Thus, there are fewer equations than unknowns.

CS exploits the principle of most of the natural signals can be expressed in a suitable basis with a small number of coefficients. Sparsity is a key requirement for the application of CS theory. However, many signals of nature are not sparse, but they can become sparse adopting a transformation. For instance, a CT image has non-zero values in most of its pixels, as opposed to his wavelet coefficients; in these basis functions, the non-zero coefficients are sparse and they contain the most important information of the original image.

Mathematically, a discrete signal $f \in \mathbb{R}^n$ can be expressed as:

$$f = \Psi x \tag{4}$$

where x is the coefficients sequence of f, and the basis Ψ is a matrix with columns φ_1, ..., φ_G. Clearly, f and x are equivalent representations of the same signal, f is a linear combination of barely F base vectors, $F << G$ [17].

In accordance with equations (3) and (4):

$$y = \Phi f = \Phi \Psi x = \Theta x \tag{5}$$

where $\Theta = \Phi\Psi \in \mathbb{R}^{M \times N}$ is the sensing matrix. The undetermined equation system in (5) causes the recuperation of x to be impossible without more information. Fortunately, in CS it is possible to solve (5) if we satisfy the condition that the measurement matrix Φ is incoherent with the sparse transformation Ψ. The incoherence means that object to be reconstructed having a sparse representation in Ψ cannot be sparse in the domain in which it was acquired. Coherence measures the highest correlation between the elements of Φ and Ψ. If Φ and Ψ contain correlated elements, coherence is high, otherwise it is low.

The condition of incoherence can preserve the information, since it requires that energy of the signal to be distributed for the entire detection domain. Each measurement has information of all the image components. Ideally, a measurement matrix ensures that relevant information on any compressible signal is not damaged by the reduced dimensionality from f to y [17], [18].

1.3. Compressive CT

A strategy to introduce CS theory in a CT configuration consists of including elements of the system that allow coding the measurements to get incoherence samples [19]. These elements are coded apertures, due to their effects on the light. Coded apertures are two-dimensional arrays with patterns of opaque materials; sections that do not contain opaque material define their transmittance, *i.e.,* the fraction of light that can pass through them. Figure 2 depicts the geometry of the sampling system for compressive CT used in this work. A system with multiple sources setting in an array including coded apertures $\mathbf{T}^1$ and $\mathbf{T}^2$, which modulate the projected beams from the i-th source to a plane with multiple detectors that measure the attenuation generated by an object f.

Figure 2. CS system for CT based on coded apertures

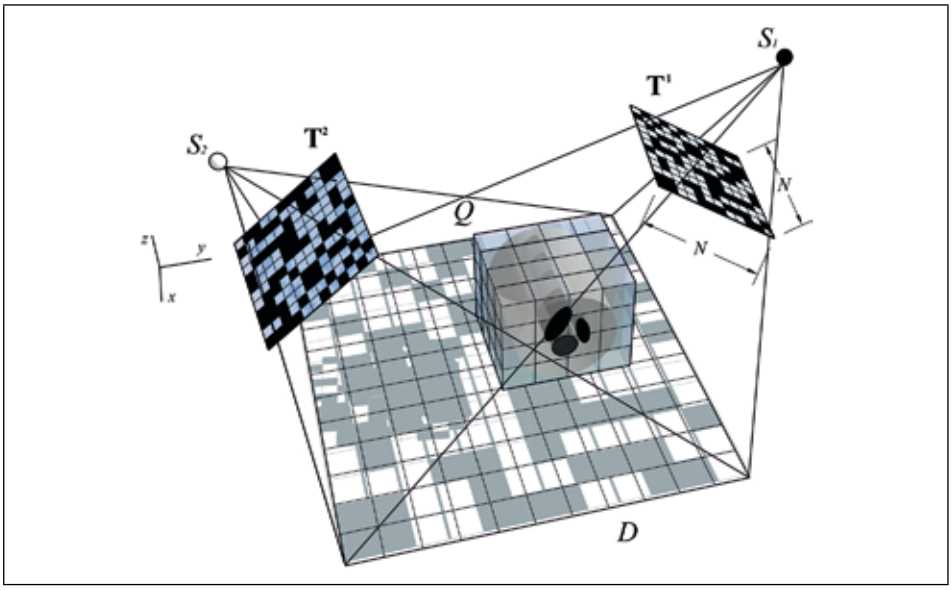

Source: authors' own presentation

In this case, the coded apertures are located between the X-ray source and the object; therefore, they modulate the energy of conical beams producing a coded projection in the detector plane. The coded aperture elements of dimensions $N \times N$, located between the i-th source S_i and the object, are denoted as $T_{xy}^i \in \{0,1\}$, where 0 blocks the X-ray beam and 1 allows it to cross . The matrix $\Phi_i = diag\left(T_{11}^i, T_{12}^i, ..., T_{NN}^i\right)$ is defined. To generalize the measurement for several sources the matrix $\boldsymbol{\Phi}$ is defined as the concatenation of the Φ_i matrices, *i.e.*, $\Phi = \left[\Phi_0 | \Phi_1 | ... | \Phi_{P-1}\right]$; and the matrix $\boldsymbol{\Phi}_i$ is the sensing matrix related with the ith source. Defining the data cube arranging in the representation basis $\boldsymbol{\Psi}$, the measurements that will be detected by the X-ray sensor can be modeled as:

$$y = \left(\sum_{i=0}^{P-1} \Phi_i \right) f = \Phi f = \Theta x \tag{6}$$

where P is the total number of sources, $\boldsymbol{\Phi}$ is the sensing matrix, and $\boldsymbol{\Theta}$ is the CS matrix for CT. Figure 3 illustrates a sampling matrix $\boldsymbol{\Phi}$ for an object of two slices of $Q_1 \times Q_3$ and a detector array of N^2 where each row represent the trajectory of a single X-ray and the grayscale values represent the different attenuation values.

Figure 3. The matrix Φ is presented for an object of two slices of $Q_1 \times Q_3 = 8 \times 8$. Grayscale pixels represent the different attenuation values in the trajectory of x-rays

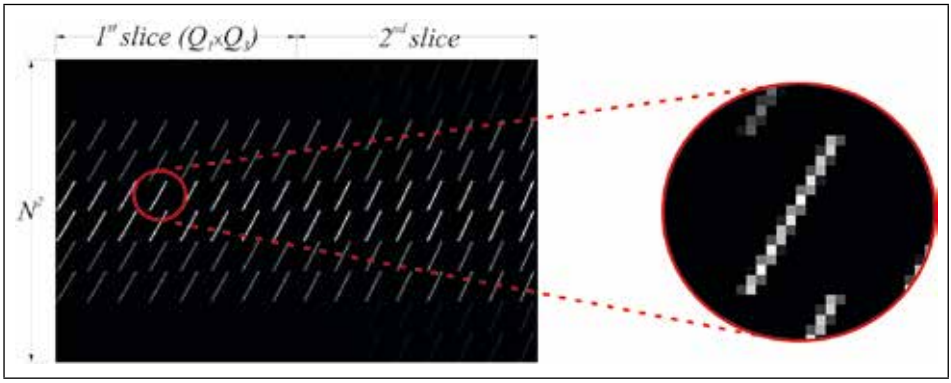

Source: authors' own presentation

If measurement in a single projection is not sufficient for reconstruction, additional projections or shots per source are required, each with a distinct coded aperture. The number of shots can be expressed in terms of the compression ratio (*Cr*) and it is defined as:

$$Cr = \frac{N_2 K}{Q} \tag{7}$$

Where K is the number of shots.

The number of sources used in the CCT configuration may vary. Also, they are disposed in an array. Figure 4 shows some examples of source distributions. Figure 4a illustrates a distribution of 2 sources on the x and *y*-axes, Figure 4b shows a distribution of 3 sources on the *x* and *y*-axes.

2. Coded Aperture Design

Coded apertures are grids with patterns of opaque materials. Transmittance is the quantity of energy that passes through an object, for this case, it is the magnitude that expresses the quantity of X-ray light that is definitely projected over an object [20]. The coded apertures have been developed and tested on X-ray systems based on fan beam geometry [21]. The coded pattern is modeled in Matlab, a mold of the aperture is printed and is filled with Tungsten powder and it is sealed with epoxy resin.

Figure 4. Different source distributions. (a) 2 sources on the x and y-axes. (b) 3 Sources on the *x* and *y*-axes

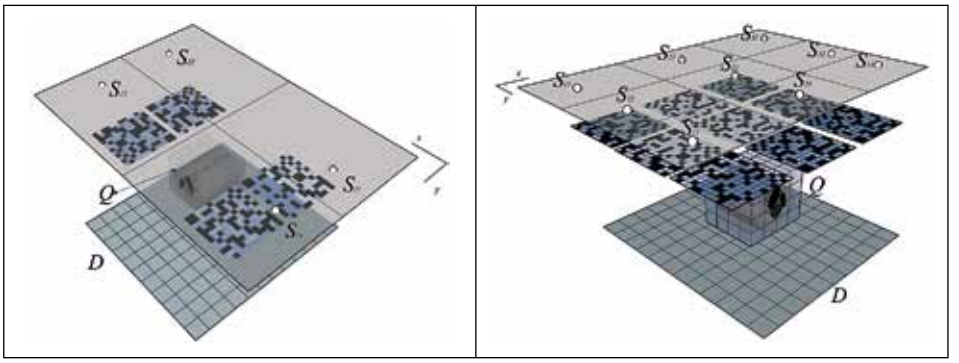

a) b)

Source: authors' own presentation

In a system based on coded apertures, the quality of reconstructions depends on the selection of the coded apertures used in the sampling. Coded apertures are traditionally used in multi-spectral signals sampling systems [22]. Coded apertures used in such systems employ type Boolean, binary, grayscale, and Hadamard random codes.

Boolean patterns where the (x, y) element of the ith coded aperture, $T_{xy}^{i} \in \{0,1\}$, have allowed getting the best results in spectral image reconstruction [20].

In this work, the Boolean pattern is employed, which not only encodes X-ray signals but also reduces the exposure of the object. The transmittance of a coded aperture is calculated as:

$$T_r^i = \sum_{x=0}^{N-1} \sum_{y=1}^{N-1} \frac{T_{xy}^i}{N^2} \tag{8}$$

Where N^2 represents the size of the coded aperture.

Figure 5 illustrates different Boolean random matrixes representing coded apertures like the ones used in this work. Figure 5a shows one coded aperture with a transmittance of 30%, Figure 5b with a transmittance of 50%, and Figure 5c with a transmittance of 70%, this means that 30%, 50% and 70% of the elements, randomly distributed, of the apertures allow light crossing, respectively.

Figure 5. Coded apertures with different transmittances (a) 30%, (b) 50% and (c) 70%

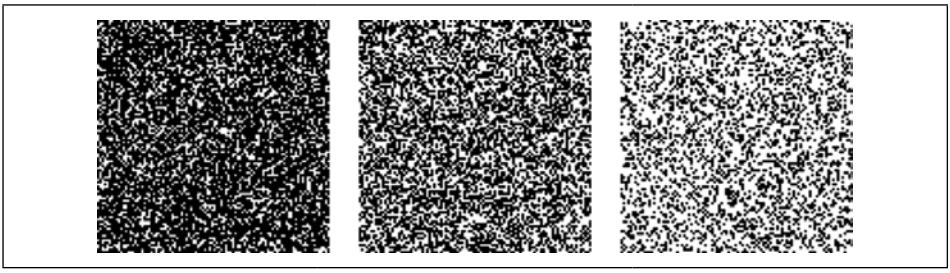

a) b) c)

Source: authors' own presentation

3. Reconstruction Methods

3.1. CT Reconstruction

The image reconstruction problem is to assign the suitable transmittance μ to each voxel in order to discretize the object. To realize such assignment, analytical or iterative methods are used. Analytical methods are the direct solution of a linear equation system; two examples of these methods are back projection and filtered back projection FBP, which is known to be very fast [1]. Iterative methods include Algebraic Reconstruction Technique (ART), and iterative algorithms, such as the Simultaneous Iterative Reconstruction Technique (SIRT) [23], [24] used in this work for comparison. The SIRT consists of three phases, executed in an iterative fashion: (1) projection of the estimated object, (2) correction factor computation (updates), and (3) back projection updates of the estimated object. The SIRT algorithm is one of many methods to solve the system of linear equations (8) by minimizing:

$$Ax = b, \tag{9}$$

Where x represents the image, b represents the projections, and A represents the scanning process.

SIRT alternates forward and back projections. Its *update equation* is:

$$x^{t+1} = x^t + CA^T R\,(b - Ax^t) \tag{10}$$

Where C and R are diagonal matrices that contain the inverse of the sum of the columns and rows of the system matrix, and the transposed matrix A^T back

projects the projection images onto the reconstruction area. Given a ray sum, it describes which pixels are hit by that ray.

For these traditional reconstruction algorithms the number of projections must satisfy the Nyquist limit to avoid streaking artifacts.

3.2. CS Reconstruction

Given a set of measurements y, which depend on the source configuration, the reconstruction of the CT projections focuses on solving a linear underdeterminate equation system by estimating f as an optimization problem. For CT reconstruction it is necessary to use algorithms that can be adjusted to converge quickly on problems of this type; in this work the results obtained with the Gradient Projection for Sparse Reconstruction (GPSR) algorithm and the TwIST algorithm are presented. The GPSR method is an algorithm used for spectral image estimation with the assumption that the signal of interest is sparse or compressible in some basis. Then the reconstruction consists on recovering x such that the cost function is minimized as

$$f = \Psi\left(\arg\min_x \left\|y - \Theta x\right\|_2^2 + \tau\left\|x\right\|_1\right) \tag{11}$$

where Ψ is a sparse representation basis, Θ is the compressive sensing matrix, x is the sparse coefficients vector, the parameter τ is a regularization constant, and $\left\|\cdot\right\|_1$ and $\left\|\cdot\right\|_2$ correspond to the l_1 y l_2 norms, respectively.

On the other side, the TwIST algorithm [25] is another framework used frequently to recover signals from compressed measurements. TwIST describes a data cube as the solution to the minimization problem:

$$\hat{f}_{TwIST}\left(\Upsilon, H\right) = \left[\frac{\arg\min}{f}\left(\frac{1}{2}\left\|y - \Theta x\right\|_2^2 + \gamma H_{TV}(x)\right)\right] \tag{12}$$

where the choices for the reguylarization function $H_{TV}(x)$ include, but are not limited to, the l_1 norm. Traditionally, TwIST uses the total variation (TV) regularizer $H_{TV}(x)$ given by

$$\sum_{k}\sum_{i,j}\sqrt{\left(x\left(i+1,j,k\right)-x\left(i,j,k\right)\right)^{2}+\left(x\left(i,j+1,k\right)-x\left(i,j,k\right)\right)^{2}} \tag{13}$$

The TV terms penalize the solution candidates with higher discrete gradients horizontally and vertically. With this regularizer the TwIST estimates the data cube, corresponding to finding a compromise between the lack of fitness of a candidate estimate to the measurement data and its degree or undesirability, given by the penalty term $\Phi_{TV}(f)$.

The TV norm measures how much an image varies across pixels so that a highly textured or noised image will have a large TV norm whereas a smooth or piecewise constant image would have a small TV norm. Finally, the parameter γ in (12) specifies the relative weight of the constraints versus the data fidelity term.

4. Simulations and Results

To show the experimental results we simulate the sampling process given a set of measurements y as in equation (3). The coded apertures are applied to eliminate a portion of the measurements. This down-sampled set of measurements is the input of the reconstruction algorithms as shown in equation (6).

Taking into account the system illustrated in Figure 2, in order to verify the CCT design, two configurations are tested. Firstly, a synthetic data cube Shepp Logan Phantom from Matlab R2015a MathWorks with images of 64×64 and 6 slices ($Q = 24576$) are used, the detector and coded aperture are configured in 64×64 pixels. Figure 6 shows some cross sections of the synthetic data cube.

Figure 6. Cross sections from synthetic data cube Shepp Logan phantom from Matlab

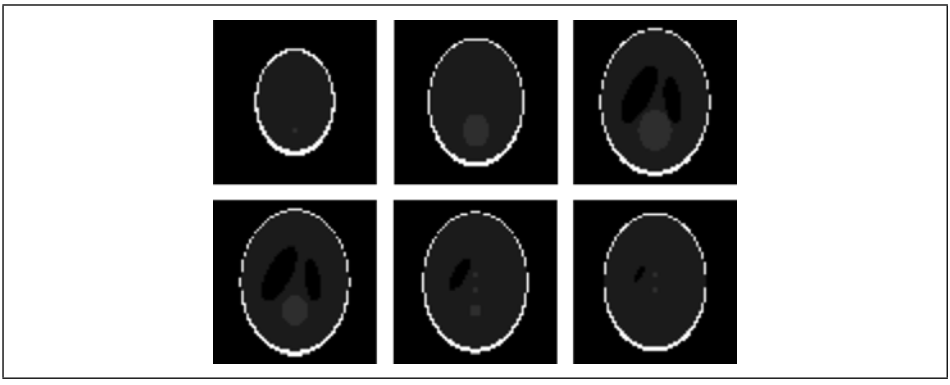

Source: authors' own presentation

Secondly, a real data cube is used from a lungs medical test; the data cube has 60 slices of 1024 × 1024 pixels. Figure 7 shows some cross sections of the real data cube. Thus, simulations to determine the effect of some parameters on the quality of reconstruction are performed.

Figure 7. Cross sections of human lungs

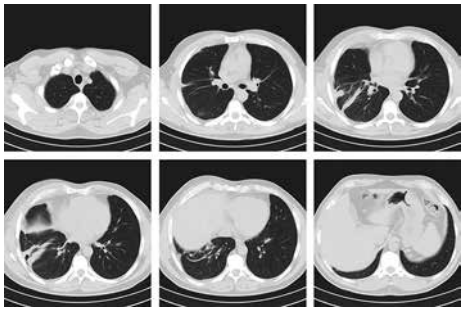

Source: Claudia Córdoba, medical radiology, 2010

The first parameter to consider was the number of sources, for this experiment coded apertures with a transmittance of 50% were used, and the compression ratio was 0.5, established because that is the mean value. The average results obtained from the reconstruction with the GPRS algorithm are presented in Table 1. In the last column, the results of 200 iterations of the SIRT algorithm are included as a traditional reconstruction reference.

Table 1. PSNR average for systems with different number of sources

source x	source y	total sources	PSNR ave. [dB]	PSNR ave. [dB] SIRT algorithm (Nyquist)
4	4	16	31.17	37.92
3	4	12	31.93	33.30
4	3	12	31.98	34.59
2	5	10	27.20	28.16
5	2	10	23.73	28.35
3	3	9	31.24	29.28
2	3	6	27.29	25.34
3	2	6	26.14	25.56
2	2	4	21.82	20.42
1	1	1	14.63	14.79

Source: authors' own presentation

As shown in Table 1, experiments were performed with different number and distribution of the sources. The best result in PSNR values is 31.98 [dB], with a distribution of 4 sources in the x-axis and 3 sources in the y-axis, a value that does not change significantly if the sources are increased in any axis due to the geometry and data cube size. These results show the effect of the number of sources on the image quality. It can be observed that 9 sources are sufficient to obtain high PSNR values with the system using a detector array of 64×64. Furthermore, it can be concluded that the results of the reconstructions with 50% of the measurements are comparable, and in some cases of higher quality, than those made with the number of measurements required for Nyquist.

For the second experiment random coded apertures were designed with different transmittance values; it is possible to find the relationship between the transmittance values of the coded apertures and the reconstruction quality. The geometry of 3×3 sources, 64×64 detector array, coded apertures, and the compression ratio of 0.5 were used for simulations. Figure 8 shows the results (in PSNR average values) obtained in ten repetitions for each specific transmittance value with random coded apertures. It shows that the simulations with the best PSNR were those corresponding to a transmittance value of 50% for the GPSR algorithm.

Figure 8. PSNR average for each transmittance value for GPSR

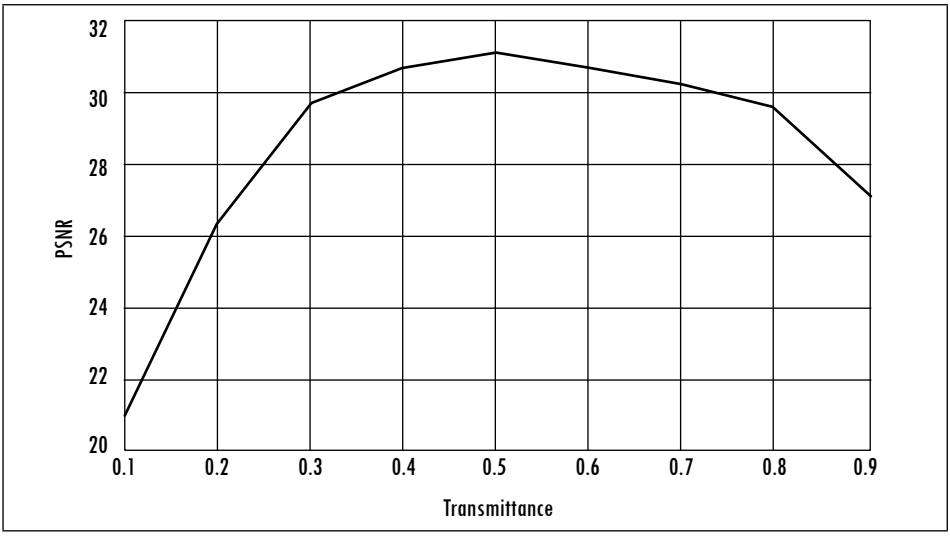

Source: authors' own presentation

Figure 9 shows the results of simulations performed for the TwIST algorithm were the best result was achieved with a transmittance value of 80%. However, it is lower than the GPSR results.

Figure 9. PSNR average for each transmittance value for TwIST

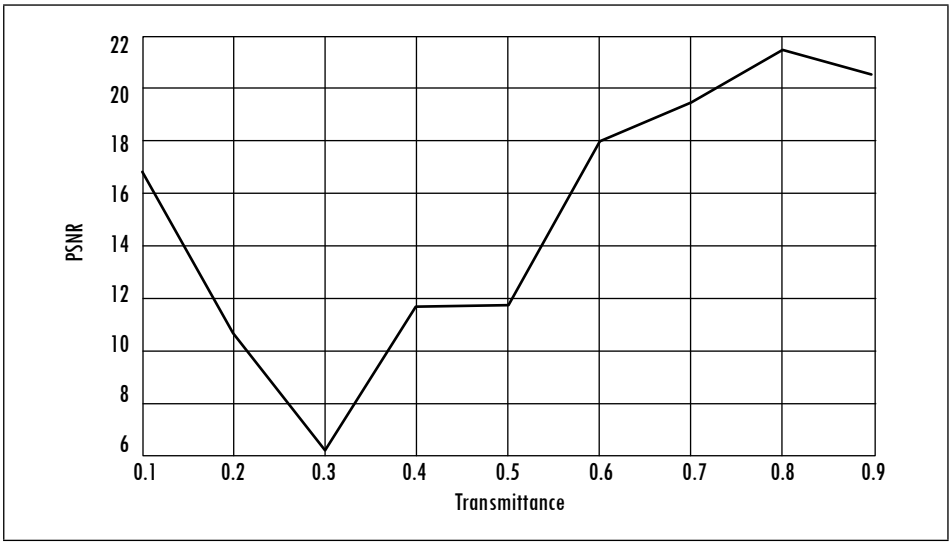

Source: authors' own presentation

Results of reconstructed cross sections of the synthetic data cube are presented in Figure 10. Figure 10a shows a cross section of the original data cube, Figure 10b shows a cross section reconstructed with the SIRT algorithm (traditional method), using a source array of 3 × 3 (PSNR = 30.01 [dB]); Figure 10c shows a cross section reconstructed with the GPSR algorithm, using a source array of 3 × 3 and coded apertures with transmittance of 50% (PSNR = 31.22 [dB]); and Figure 10d shows a cross section reconstructed with the TwIST algorithm, using a source array of 3 × 3 and coded apertures with transmittance of 80% (PSNR = 21.46 [dB]). It can be noted the quality of the reconstructed image with the GPSR algorithm is higher than the quality obtained by other algorithms.

In addition, in Figure 11 reconstructed cross sections from a real data cube of a human patient thorax are shown. The configuration used for this slice was a detector matrix of 128 × 128 and 9 sources, and the compression ratio was 0.33 as it is shown in Figure 4b. Figure 11a shows a cross section of the original data cube. Figure 11b shows a cross section reconstructed with SIRT algorithm

(Nyquist), PSNR=33.37 [dB]. Figure 11c shows a cross section reconstructed with GPSR algorithm, transmittance of 50% and PSNR=35.07 [dB].

Figure 10. Comparison between a cross section of the original cube and a cross section reconstructed with 9 sources

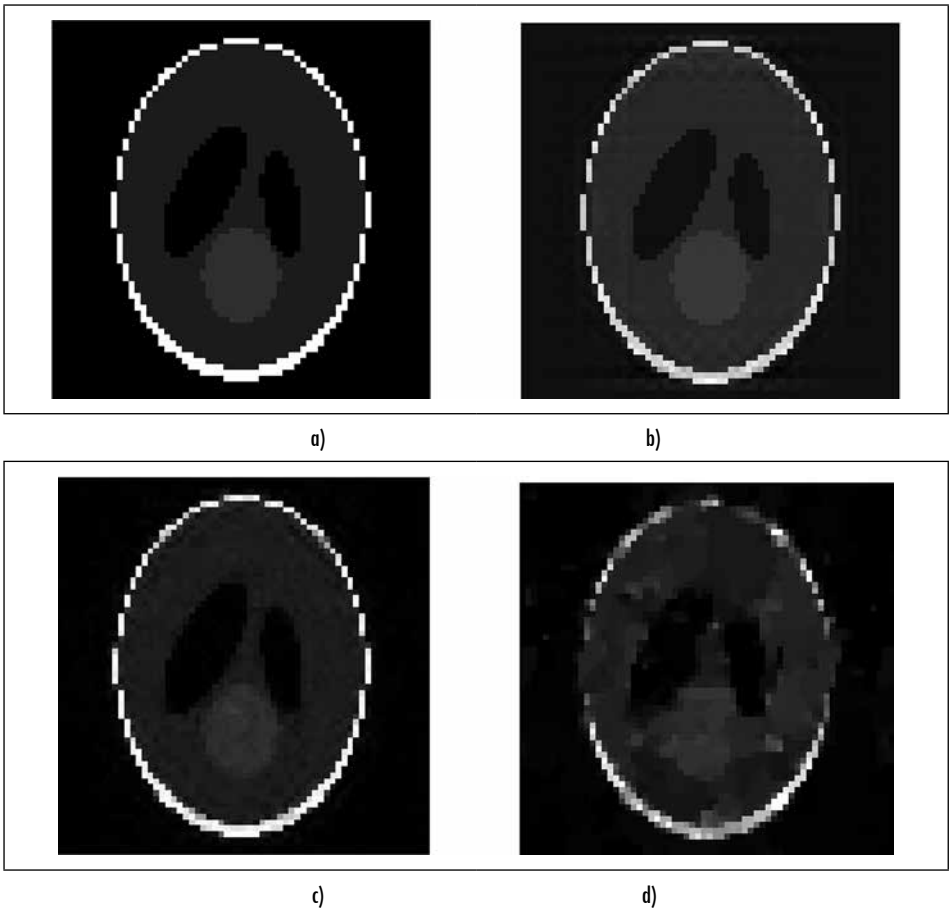

Note. (a) Cross section of the original data cube. (b) Cross section reconstructed with SIRT algorithm (Nyquist), PSNR=30.01[dB]. (c) Cross section reconstructed with GPSR algorithm , transmittance of 50% and PSNR=31.22 [dB]. (d) Cross section reconstructed with TwIST algorithm, transmittance of 80%, and PSNR=21.46 [dB].
Source: authors' own presentation

Table 2 shows the results of simulations for different compression ratios with the GPSR algorithm. It can be seen that the quality of reconstruction with 4 and 9 sources increases while with 1 source remains unchanged. It can be observed in Table 2 that the image quality increases when more measurements are used.

Figure 11. Comparison between cross sections from a real data cube from a human thorax reconstructed from a configuration of 128 × 128 detectors and 3 × 3 sources

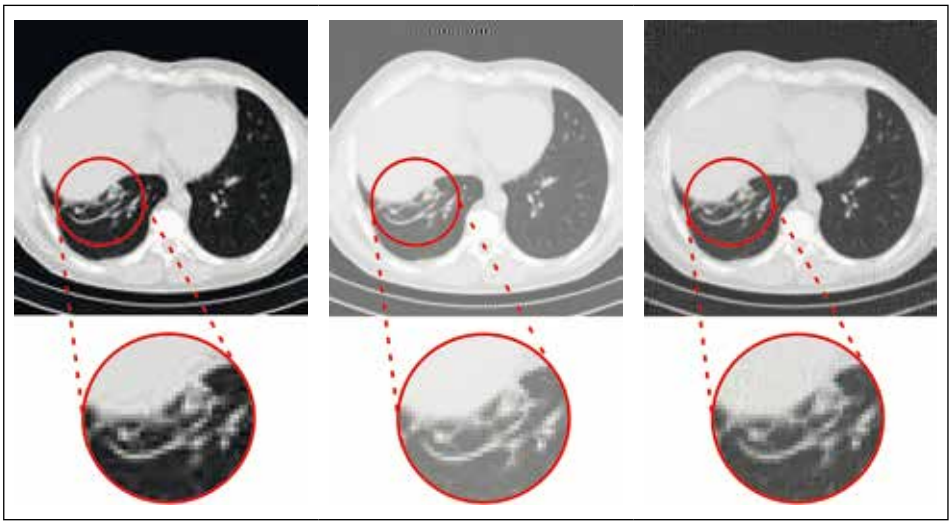

a) b) c)

Note. (a) Cross section of the original data cube. (b) Cross section reconstructed with SIRT algorithm (traditional), PSNR=33.37 [dB]. (c) Cross section reconstructed with GPSR algorithm, transmittance of 50% and PSNR=35.07 [dB].
Source: authors' own presentation

Table 2. PSNR average for systems with different number of sources and shots

Sources	Cr	1×1	2×2	3×3
Shots			PSNR ave. [dB]	
2	0.33	14.63	21.82	31.24
3	0.50	14.67	24.72	33.45
4	0.66	14.63	25.17	34.28

Source: authors' own presentation

5. Discussion

The compressive sensing technique allows compressing a signal at the acquisition step by using different sample patterns and the projections needed to recover data are less than the Nyquist rate. Some previous works have focused on developing models for joining CS to CT, nevertheless, it has not been detailed the measurement architectures design to improve the quality of the reconstructions. We have proposed a multisource CT system for measuring coded projections physically by using coded apertures. It is demonstrated that physical coding can be used for data compression in CT.

Simulations indicate that the compressive CT architecture provides comparable results to those achieved with traditional CT architectures and the reconstruction algorithms used for CS require a fewer number of measurements than traditional algorithms used in CT to obtain comparable results.

In this work it was found that the number of sources, their distribution and the transmittance of coded apertures are important factors that largely define the quality of reconstructions. Additionally, with the result of simulations, it was found that the transmittance with the best results obtained is 50% and the corresponding average PSNR is 31.01 [dB].

Acknowledgments

The authors gratefully acknowledge the Vicerrector de Investigación y Extensión of Universidad Industrial de Santander for supporting this work registered under the project titled "Diseño y simulación de una arquitectura de tomografía computarizada para el sensado compresivo de imágenes de rayos-X" (VIE code 1803).

References

[1] T.M. Buzug, *Computed Tomography: From Photon Statistics to Modern Cone-Beam CT*. Berlin: Springer-Verlag, 2008.

[2] S. Chen, H. Chen, S. Li, J. Li, and S. Li, "Evaluation measurement of accuracy of industrial computed tomography," *Nondestructive Evaluation/Testing: New Technology & Application (FENDT), 2013 Far East Forum on*, Jinan, pp. 177-180, 2013.

[3] V. Cnudde and M.N. Boone, "High-resolution X-ray computed tomography in geosciences: A review of the current technology and applications," *Earth-Sci. Rev*., vol. 123, pp. 1-17, 2013.

[4] J. Dewanckele, T. De Kock, G. Fronteau, H. Derluyn, P. Vontobel, M. Dierick, L. Van Hoorebeke, P. Jacobs, V. Cnudde, "Neutron radiography and X-ray computed tomography for quantifying weathering and water uptake processes inside porous limestone used as building material," *Mater. Charact*., vol. 88, pp. 86-99, 2014.

[5] Shannon, C. E., "Communication in the presence of noise," in Proc. of the IEEE, vol. 86, no. 2, pp. 447–457, 1998.

[6] R. Smith-Bindman, J. Lipson, R. Marcus, K.-P. Kim, M. Mahesh, R. Gould, A. Berrington de González, and D. L. Miglioretti, "Radiation dose associated with common computed tomography examinations and the associated lifetime attributable risk of cancer," *Arch. Intern. Med*., vol. 169, pp. 2078–86, 2009.

[7] A. Wagadarikar, R. John, R. Willett, and D. Brady, "Single disperser design for coded aperture snapshot spectral imaging," *Appl. Opt*., vol. 47, pp. B44–51, 2008.

[8] D. L. Donoho, "Compressed sensing," *IEEE Trans. Inf. Theory*, vol. 52, pp. 1289–1306, 2006.

[9] E. Maire and P.J. Withers, "Quantitative X-ray tomography," *Int. Mater. Rev.*, vol. 59, pp. 1–43, Jan. 2014.

[10] K. Choi and D. J. Brady, "Coded aperture computed tomography," in *Proc. SPIE 7468*, vol. 7468, p. 74680B–74680B–10, 2009.

[11] M.M. Sevak, F.N. Thakkar, R.K. Kher, C.K. Modi, "CT image compression using compressive sensing and wavelet transform," *Int. Conf. on Communication Systems and Network Technologies*, pp. 138–142, 2012.

[12] G. Wang, H. Yu, and B. De Man, "An outlook on x-ray CT research and development." *Med. Phys.*, vol. 35, pp. 1051-1064, 2008.

[13] E. Niemi, M. Lassas, A. Kallonen, L. Harhanen, K. Hämäläinen, and S. Siltanen, "Dynamic multi-source X-ray tomography using a spacetime level set method," *J. Comput. Phys.*, vol. 291, pp. 218-237, 2015.

[14] E. Niemi, M. Lassas, and S. Siltanen, S., "Dynamic X-ray tomography with multiple sources," in *Image and Signal Processing and Analysis (ISPA), 2013 8th International Symposium on*, pp. 618-621, 2013.

[15] O. Espitia, Y. Mejía, and H. Arguello, "Tomografía computarizada: proceso de adquisición, tecnología y estado actual," *Tecnura*, vol. 20, no. 47, pp. 119-135, 2016.

[16] S. Qaisar, R.M. Bilal, W. Iqbal, M. Maureen, and S. Lee, "Compressive sensing: From theory to applications, a survey," Commun. Networks, vol. 15, pp. 443–456, 2013.

[17] M. B. Wakin, "An introduction to compressive sampling," *IEEE Signal Process. Mag.*, vol. 25, no. 2. pp. 21–30, 2008.

[18] E. J. Candes, J. Romberg, and T. Tao, "Robust uncertainty principles: Exact signal frequency information," *IEEE Trans. Inf. Theory*, vol. 52, pp. 489–509, 2006.

[19] E. J. Candes and T. Tao, "Near-optimal signal recovery from random projections: Universal encoding strategies," *IEEE Trans. Inf. Theory*, vol. 52, pp. 5406–5425, 2006.

[20] G.R. Arce, D.J. Carin, H. Argüello, and D.S. Kittle, "Compressive coded aperture spectral imaging: An introduction," *IEEE Signal Process. Mag.,* vol. 31, no. 1, pp. 105–115, 2013.

[21] K. P. MacCabe, A.D. Holmgren, M.P. Tornai, and D.J. Brady, "Snapshot 2D tomography via coded aperture X-ray scatter imaging.," *Appl. Opt.*, vol. 52, no. 19, 2013.

[22] D.F. Galvis, Y.H. Mejía, and H. Argüello, "Efficient reconstruction of Raman spectroscopy imaging based on compressive sensing," *DYNA*, vol. 81, no. 188, pp. 116–124, 2014.

[23] F. Xu, W. Xu, M. Jones, B. Keszthelyi, J. Sedat, D. Agard, and K. Mueller, "On the efficiency of iterative ordered subset reconstruction algorithms for acceleration on GPUs.," *Comput. Method Prog. Biomed*, vol. 98, no. 3, pp. 261–270, 2010.

[24] Má. A. T. Figueiredo, R. D. Nowak, and S. J. Wright, "Gradient projection for sparse reconstruction: Application to compressed sensing and other inverse problems," *IEEE J. Sel. Top. Signal Process.*, vol. 1, no. 4, pp. 586–597, Dec. 2007.

[25] J.M. Bioucas-Dias and M. a T. Figueiredo, "A new twIst: two-step iterative shrinkage/thresholding algorithms for image restoration," *IEEE Trans. Image Process*., vol. 16, no. 12, pp. 2992–3004.